13th ECNDT 3-7 JULY 2023 | LISBON

Discovery and validation of the North Face Corridor in the Great Pyramid of Giza using non-destructive techniques

Mohamed Elkarmoty[1*], Khalid Helal[1], Hussien Allam[2], Mohamed Ali[2], Mohamed Sholqamy[1], Amr Elbakri[1], Randa Deraz[2], Polina Pugacheva[3], Johannes Rupfle[3], Jochen Kollofrath[3], Clarimma Sessa[3], Olga Popovych[3], Benedikt Maier[3], Alejandro Ramirez Pinero[3], Thomas Schumacher[4] ,Sébastien Procureur[5], Hector Gomez[5], David Attié[5], Irakli Mandjavidze[5], Patrick Magnier[5], Benoit Marini[6,7], Pierre Gable[8], Emmanuel Guerriero[8], Nicolas Serikoff[6], Jean-Baptiste Mouret[9,], Bernard Charlès[10], Marion Lehuraux[5], Théophile Benoit[5] , Denis Calvet[5], Xavier Coppolani[5], Mariam Kebbiri[5], Philippe Mas[5], Simon Bouteille[11], Kunihiro Morishima[12,13], Mitsuaki Kuno[13], Akira Nishio[13], Nobuko Kitagawa[13], Yuta Manabe[13], Fumihiko Takasaki[14], Hirofumi Fujii[14], Kotaro Satoh[14], Hideyo Kodama[14], Kohei Hayashi[14], Shigeru Odaka[14], Yoshikatsu Date[15], Makiko Sugiura[16], Hamada Anwar[17], Mehdi Tayoubi[6,10], Hany Helal[1,6]& Christian U. Grosse[3]

1 Department of Mining, Petroleum, and Metallurgical Engineering, Faculty of Engineering, Cairo University, Gamaa Street 1, Giza, 12613, al-Giza, Egypt.

2 Rock Engineering Laboratory, Faculty of Engineering, Cairo University, Gamaa Street 1, Giza, 12613, al-Giza, Egypt.

3 Chair of Non-destructive Testing, TUM School of Engineering and Design, Technical University of Munich, Franz-Langinger-Str. 10, Munich, 81245, Bavaria, Germany.

4 Civil and Environmental Engineering, Portland State University, 1930 SW 4th Avenue, Portland, 97201, Oregon, USA.

5 IRFU, CEA, Université Paris-Saclay, F-91191 Gif-sur-Yvette, France.

6 Heritage Innovation Preservation Institute (HIP Institute), 50 Rue de Rome, Paris, 75008, Île-de-France, France.

7 Whatever The Reality, 5 Chemin de Picurey, 33520 Bruges, France.

8 Emissive, 71 rue de Provence, 75009 Paris, France.

9 Université de Lorraine, CNRS, Inria, F-54600, France.

10 Dassault Systèmes, 10 Rue Marcel Dassault, 78140 Vélizy-Villacoublay, France.

11 IRIS Instruments, France.

12 PRESTO, Japan Science and Technology Agency (JST), Saitama 332-0012, Japan.

13 Nagoya University, 1 Furo, Chikusa, Nagoya, Aichi, 464-8602, Japan.

14 High Energy Accelerator Research Organization (KEK), 1-1 Oho, Tsukuba, Ibaraki 305-0801, Japan.

15 NHK Enterprises, Japan.

16 Suave Images, Japan.

17 Freelance logistics coordinator, Egypt.

Abstract

In 2017, ScanPyramids project (www.scanpyramids.org) published a paper in Nature (Morishima et al., 2017) revealing the discovery of a big void (ScanPyramids Big Void BV) observed with nuclear emulsion films (Muography), it has a cross-section similar to that of the Grand Gallery and a minimum length of 30 meters situated above the Grand Gallery. In addition, a geometrically non-identified void in the Northern Face of the Pyramid (ScanPyramids Northern Face Corridor SP-NFC) was detected as well in 2017 followed by further detailed and focused muography measurements up to 2022 (Morishima and Procureur et al., 2023). ScanPyramids SP-NFC corridor has been investigated in more detail with a wider set of non-destructive techniques. The result of GPR, Ultrasonic and image fusion detected precisely the location and shape of ScanPyramids SP-NFC (Elkarmoty and Rupfle et al.,2023). In this paper, we present overview on the application of Muography, Ground Penetrating Radar, Ultrasonic Tomography, and Electrical Resistivity Tomography on the Chevron of the Great Pyramid where ScanPyramids SP-NFC is located behind. The objective of the NDT measurements is to detect the geometry, location, orientation, and extension of ScanPyramids SP-NFC with more than one NDT method. The paper addresses the validity and limitations of each method used providing the limitations of each technique in this particular case study.

KEYWORDS: Great Pyramid, Non-Destructive Testing, Cosmic-Ray Muons, Ground Penetrating Radar, Electric Resistivity Tomography, Ultrasonic, Image Fusion, ScanPyramids.

*mohamed.elkarmoty@cu.edu.eg (crosspending author)

https://doi.org/10.58286/28180

1. Introduction

The Great Pyramid (also known as Khufu's Pyramid) in Egypt is one of the oldest and largest stone buildings still standing (Figure 1). Over 2.3 million limestone stones weighing a total of roughly 6.4 million tonnes were used to create the building, which was originally 148 meters tall (though it is now just 139 meters) and 231 meters wide. Despite being one of the Ancient World's Seven Wonders, it continues to be a mystery. Researchers, Egyptologists, and archaeologists have proposed a number of theories regarding the construction of this pyramid. None of them, however, have been supported by evidence up to this point. The ScanPyramids mission (www.scanpyramids.org) began scanning the Great Pyramid in October 2015 using cutting-edge technology. Using cosmic-ray muon radiography analysis, ScanPyramids Big Void (SP-BV) was declared in November 2017 [1]. On the northern face of the Pyramid, behind the so-called Chevron (Figure 1), muon measurements also suggested the presence of an anomaly, most likely an unrecognized corridor known as the ScanPyramids North-Face Corridor (SP-NFC) [2]. For more accurate localization of this anomaly, a combination of NDT techniques (GPR, ERT, Ultrasonic, and Image Fusion) was used, based on the results from GPR, Ultrasonic, and Image Fusion, the location and geometry of the north face corridor anomaly was detected with few centimeters accuracy [3].

The main objective of this article is to summarize our experience in applying various NDT techniques for the investigation of the internal structure of the Khufu Pyramid from 2014 till now with illustrations of the advantages and limitations of the different techniques.

Figure 1: Overview of the great pyramid of Giza and its Chevron.

2. Non-destructive Techniques

2.1. Muography

Recently muography observations were made using three different cosmic ray muon measurement techniques: scintillation detectors, gas detectors, and nuclear emulsion plates. The nuclear emulsion plates were observed simultaneously from multiple points by installing detectors at two locations, inside the descending corridor and the Queen's Chamber (Figure 2). As a result of observations from the descending corridor, an unknown passage-like structure was discovered in 2016 above the descending corridor and behind the Chevrons, and was named ScanPyramids North Face Corridor (SP-NFC). In order to estimate the detailed location of the discovered structure and its three-dimensional shape, including its cross-section and inclination, we conducted multi-point observations by installing nuclear emulsion plates inside the descending corridor and at multiple points in the al-Ma'mun corridor (Figure 2). Furthermore, as a result of observations from the Queen's Chamber, we discovered in 2017 that an unknown structure of the same size as the Grand Gallery is located above it, and we named this new structure the ScanPyramids Big Void (SPBV) [1] [4]. The nuclear emulsion plates were only able to maintain their performance for about one month during the initial phase of the ScanPyramids. However, we succeeded in improving the long-term performance by adjusting the compounds added to the nuclear emulsion plates, and now, under the pyramid's constant temperature environment of 25°C, continuous observation for several months is possible. At the same time, improvements in nuclear emulsion plate manufacturing technology have made it possible to simultaneously install nuclear emulsion plates as large as 10 square meters inside the pyramids. As a result, nuclear emulsion plates were installed and covered many locations inside the pyramid.

Figure 2: Nuclear emulsion detectors installed in the Pyramid of Khufu.

Gaseous detectors were first developed for particle physics experiments, with several important modifications allowing them to be used in harsh conditions and around the public. In spite of the required compactness, the excellent accuracy of the detector ensured an angular resolution below 1 mrad. The most challenging measurements took place outside in 2016-2017 (Figure 3a), as the telescopes had to cope with large temperature fluctuations, wind, and dust. In spite of these difficulties, they were able to detect a first void of a few meters at a distance of 150 m, a performance never achieved before in muography. They were later able to detect the Big Void in front of the North face, providing the very first observation of a void in the core of a pyramid from the outside using non-destructive techniques. In order to better investigate the characteristics of this void, the telescopes were later installed in the Grand Gallery (2018-2019), see Figure 3b. A last measurement campaign took place in 2019-2020 in order to better localize the North Face Corridor. A rough 3D reconstruction could be obtained which confirmed the existence of this void without any use of numerical simulations which could lead to bias in the analysis. The muography technique concluded that the location of the SP-NFC is located in the center of the Chevron with cross-section of 2 m x 2m, and ends at 9.0 m southward. A smaller corridor of less than 1.0 m between these two structures cannot be completely ruled out from these measurements [2].

(a) (b)

Figure 3: The muon telescopes, (a) during their installation outside and (b) in the Grand Gallery.

2.2. GPR

The GPR measurements were conducted over the chevron area between 2020-2022 [3]. The main objective was to precisely localize the SP-NFC and to determine its dimension. Over two successive years, different GPR antennae with different frequencies were used to stand on the optimum frequency for this objective in terms of resolution and penetration depths. To be able to carry out the planned GPR measurements, scaffolding was needed to give the team an access to the different levels of the chevron. Regarding the GPR measurements (Figure 4a), scanning had been started using an antenna from GSSI of a 300-800 MHz dual frequency, an antenna from IDS of a 200-600 MHz dual frequency, and a GSSI 400 MHz antenna. For the GSSI 300-800 MHz antenna, a grid (50 cm spacing) was constructed. The results showed a zone of strong reflections at the middle of the chevron slightly to the right (Figure 4b), but it was difficult to determine the exact location and shape of these anomalies as the grid was relatively large and the attenuation of the signal was high. Consequently, a narrower frequency band antenna (200-600 MHz) was used to reduce signal attenuation and to construct a denser grid (20 cm spacing). This dense grid resulted in a clearer location of the anomaly, and it was dense enough to build a 3D representation with adequate resolution (Figure 4c). However, the resolution wasn't good enough to define the exact dimension of the found corridor-shaped anomaly. So, a denser grid (10 cm spacing) with quite a higher frequency was constructed using the GSSI 400 MHz antenna. The obtained reflections were better and led to a higher-resolution 3D representation of the data (Figure 4d).

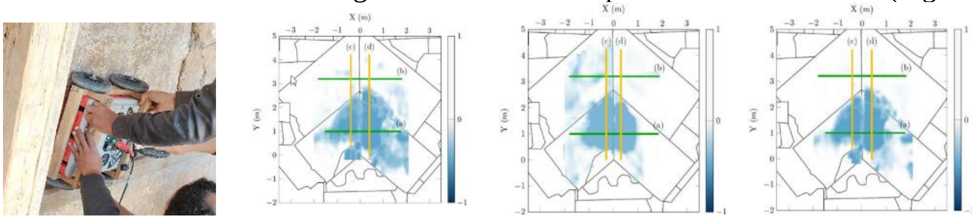

(a) (b) (c) (d)

Figure 4: (a) The field measurements, (b) 3D results of the 200 MHz, (c) 3D results of the 400 MHz, and (d) 3D results of the 600 MHz (Elkarmoty and Rupfle et al.,2023).

In this case study, it was counted on the GPR in precisely determining the exact location of the air anomaly on the north face of the great pyramid. But, due to the high wave attenuation in such a blocky medium, and the deteriorated surface, the penetration depth was limited. Moreover, the frequency range of any antenna dictates its size and depth capability. The above-mentioned limitations can explain why it was difficult to count on this technique in determining the end of the air anomaly, however it detected in more precision the location and shape of SP-NFC. It was found behind the lower two blocks of the Chevron, with a chevron-shaped ceiling, a width of 2.1 m, and a maximum height of 2.3 m [3].

2.3. UST

The UST measurements performed on the chevron area were challenging because of the large thickness of the blocks up to over 1 m, the presence of many joints, and the deterioration of the surface on some of the blocks. For the measurements, state-of-the-art UST equipment (Screening Eagle Technologies Pundit PD8000) was employed. A multi-channel pulse-echo array system was used to investigate the area of the chevron by measuring UST profiles in vertical and horizontal directions (Figure 5). Ultrasonic waves can be used to accurately locate and determine the shape of hidden voids, anomalies, cracks, or discontinuities inside a medium such as limestone. Drawbacks of ultrasonic testing include the achievable penetration depth within the blocks and the high attenuation of the signal behind an air gap, e.g., the joint with the posterior blocks, as the energy of the transmitted stress waves through such boundaries is so low that its reflection may not be detectable by the device. Furthermore, the wave velocities in the measured objects may be highly influenced by the roughness and deterioration of the block's surface. Finally, another disadvantage of UST is the requirement for more time for each measurement, as the device must be kept in place until the signal stabilizes.

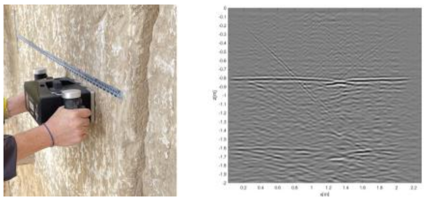

(a) (b)

Figure 5: The Ultrasonic measurements at the chevron(a) Field measurements, (b) Ultrasonic profile.

For the measurements at the Great Pyramid, two eight-channel ultrasonic shear wave arrays were employed that could be combined to form a 16-channel array, which increases the recorded number of A-Scans at a given measurement location, this results in a higher signal-to-noise ratio (SNR) due to the higher wave ray path density. The augmented SNR enables the visualization of a reflector at higher depths, where the amplitude of the reflected signal is low. The Ultrasonic results confirmed the borders of the anomaly (SP-NFC) detected by GPR, as well as confirming the different thicknesses of the lower blocks as detected by GPR as well.

2.4. ERT

In this study, Electrical Resistivity Tomography (ERT) was applied to estimate the size, shape, and position of the void behind the Chevron. One difficulty in the measurements made over dry rock is the high electrode contact impedance caused by the contrast in resistance between the electrode and the medium. The electrodes should be light to be fixed in vertical positions on the walls and flexible to conform to the uneven rock surface. So, the so-called mesh electrodes were used [5], to meet all these requirements, consisting of a square steel-made plate with a surface area of 0.20×0.20 m (Figure 6a). Galvanic contact with the rock's surface was achieved by using a sponge moistened with fresh water. The data was measured along ten parallel profiles with 0.75 m electrode spacing, and inter-line distances of 0.25 m (Figure 6b). The findings of the ERT study have to be seen in light of some limitations. The topographic complexity of the investigated area and limited working space were the major constraints for the ERT survey. First, they affect the depth of investigation, which largely depends on the total length of the transmitting line. Moreover, the height differences between chevrons and stone blocks located on the flanks of the study area reached two meters. This can have an adverse effect on the propagation of electric current, impairing its penetration depth. In our study, the maximum available line length on-site was 9.42 meters. Based on the estimate of the model's coverage, it can be assumed that in the upper parts of the inversion model (on average, down to a depth of 2 m), the resistivity is well explained by the data.

(a) (b)

Figure 6: (a) The mesh electrodes used, and (b) the ERT survey line on the Chevron blocks.

The resolution is influenced by the density of measurements (electrode and inter-line spacing), the inversion parameters (mesh size, smoothing constraints), measurement errors, and the characteristics of the study area, for example, the presence of strong resistivity contrasts. The data were inverted over a fine mesh using such inversion parameters to increase resolution. It should be emphasized that the complex 3D resistivity distribution that exists in our case can best be reproduced in a 3D model that considers the topography of the Chevron Zone and adjacent areas. The 3D ERT results showed unidentified air anomalies behind the Chevron that will be published in more detail after finishing the analysis of results.

2.5. Image Fusion

Image fusion (IF) was employed to merge reconstructed GPR and UST images. For our case where the coordinate systems were the same, registration involved translating the GPR image to align the direct wave with the surface, resampling both images to have the same size and resolution, and normalizing the intensities. The selected pixel size was 2.5 x 2.5 mm, which allows sufficient sampling of the shortest wavelengths contained in the image of 28 mm (UST image). The GPR image was kept in color and the UST image was in greyscale. The two registered images were merged using a Wavelet-based fusion algorithm available in MATLAB [6]. The algorithm decomposes the two images into approximations and details coefficients [7]. For this study, the db2 wavelet with a decomposition level of five was used and fusion was performed by taking the minimum and maximum of the approximations and details, respectively. A sample fused image is shown in Figure 7. The location of the profile is at Y = 1.40 m and spans across Blocks 3 and 4 (see Figure 7). Reflectors A and A' represent the backwalls of Blocks 3 and 4, respectively. B is a shallow reflector that is only visible in the UST data in this profile. The diagonal reflectors (C and C') and the parabolic reflectors (D and D') are the results of the joint located at X = 0.0 and the back corners between Blocks 3 and 4, respectively. In this representation, the information from the GPR profile provides a colored background and the UST profile introduces topographic-like features, which make the figure visually appealing and straightforward to interpret. These results demonstrate that image fusion is not only possible in a cultural heritage setting like the limestone of the Great Pyramid, but it also allows for confirming measurement variables as well as improving the interpretation of NDT results. Some of the challenges of this technique are selecting appropriate registration and fusion parameters and algorithms since this approach has not been employed in this setting.

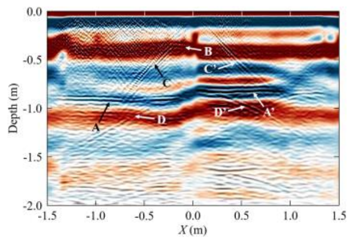

Figure 7: Sample fused GPR/UST image for a horizontal profile at Y=1.40 m, spanning across Blocks 3 and 4 (Elkarmoty and Rupfle et al.,2023).

3. Conclusion

The main aim of this paper is to demonstrate the ability to apply different NDT techniques (Muons, GPR, UST, ERT, Image fusion of results) in exploring the internal structure of the great pyramid with illustrations of the advantages and limitations of each technique. So far, using various NDT techniques two main anomalies were detected in the Great Pyramid of Giza, the big void above the Grand Gallery (SP-BV) and the North-Face Corridor anomaly (SP-NFC). The demonstration and comparison focused mainly on the SP-NFC anomaly. Using three different muon detectors (Nuclear emulsion plates, Scintillation detectors, and Gas detectors) the SP-NFC anomaly was confirmed but there's a limitation regarding knowing the precise shape of such a

void and the inability to resolve the cross-section of the corridor (trapezoid, rectangular, etc.), however, it provided the best 3D detection of the anomaly, particularly the internal extension. The GPR measurements were carried out using 3 different frequencies with different grid spacings (50, 20, 10 cm), the SP-NFC anomaly was detected with all the different antennae but the best resolution for the 3D localization of the anomaly resulted from a dense grid spacing (10 cm) and using 400 MHz antenna although it was difficult to determine the end of the air anomaly using GPR solely. The ultrasonic technique also confirmed the location of the NFC anomaly but there's a limitation to this technique regarding the attenuation of the signal after the air boundaries which led to the inability of detecting the end of the void. The ERT technique was adapted also to be applied for such a complex geometry and the analysis of results is still in progress. The image fusion approach was used for better visualization, correlation, and interpretation between GPR and UST techniques, and the interpretation of results was improved successfully.
Figure 8 represents a comparison between the different proposed geometries of SP-NFC detected using different NDT techniques. It can be seen that the use of one NDT technique is not enough for accurately detecting the location, shape, dimension, and extension of such anomalies in a complex geometry structure such as the great pyramid because each technique has its advantages and limitation.

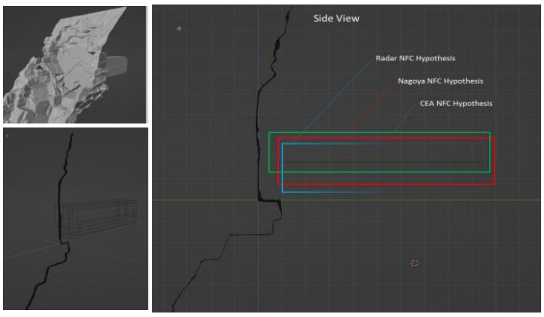

Figure 8: The proposed location, geometry, and extension of the NFC anomaly (Radar (GPR), Nagoya (nuclear emulsion films), and CEA (gaseous detectors)).

Acknowledgments:
GPR, UST and ERT measurement campaigns were supported by TUM International Graduate School of Science and Engineering (IGSSE) as well as by the German Academic Exchange Service (DAAD) in the scope of the "German-Egyptian Progress Partnership, Program Line 2" under the title "Non-Destructive Techniques for the Preservation of Egyptian Cultural Heritage ". We acknowledge the Science, Technology & Innovation Funding Authority (STDF) for funding the establishment of a new center of excellence in Non-destructive Techniques & Engineering Geophysics at Cairo University - Faculty of Engineering providing the equipment used in this research. Special thanks are due to the Supreme Council of Antiquities and the Egyptian Ministry of Tourism and Antiquities for permitting the work of ScanPyramids mission in cooperation with and under supervision of the Supreme Council of Antiquities. We thank Mr. Ahmed Issa (Minister of Tourism and Antiquities), Dr. Mamdouh Eldamaty and Dr. Khaled El-Enany (Former Ministers of Tourism and Antiquities), Dr. Mostafa Waziry (Secretary General of the Supreme Council of Antiquities), the Scientific Archaeological Committee headed by Dr. Zahi Hawass, Mr. Ashraf Mohy (Director of the Pyramids Archaeological Area) and Dr. Nashwa Gaber (General Supervisor of Foreign Missions and the Permanent Committee), and their collaborators and assistants. Thanks to the management of Cairo University and Faculty of Engineering - Cairo University for the support of ScanPyramids project. Special thanks to Jean-Pierre Houdin who transmitted his passion for the Great Pyramid to many members of the project. Dr. Ing. Klaus Mayer and Karl-Josef Sandmeier advised on ultrasound and Radar data reconstruction, data analysis, and numerical simulations. Support in different phases of the project by Mr. Johannes Scherr, Eng. Mostafa Ameen, Eng. Khaled Abdelghafar, Prof. Dr. Ernst Rank, and Prof. Dr. Barbara Wohlmuth is gratefully acknowledged. The result of this research is part of the ScanPyramids project, which is supported by: NHK, Suez, le Groupe Dassault, Batscop, Itekube, Parrot, ILP, Kurtzdev, GenG, Schneider Electric and also la Fondation Dassault Systèmes which has provided unfailing support since the starting of the project.

References:
1. Morishima et al., 2017, "Discovery of a big void in Khufu's Pyramid by observation of cosmic-ray muons". Nature 552, 386-390.
2. Morishima and Procureur et al., 2023, "Precise characterization of a corridor-shaped structure in Khufu's Pyramid by observation of cosmic-ray muons". Nature Communications 14, 1144
3. Elkarmoty and Rupfle et al.,2023, "Localization and shape determination of a hidden corridor in the Great Pyramid of Giza using non-destructive testing" , NDT & E international, 102809, ISSN 0963-8695.
4. Morishima et al., 2022, "Development of Nuclear Emulsions for Muography", Muography: Exploring Earth's Subsurface with Elementary Particles, chapter21.
5. Tomaškovičová et al., 2016. Effect of electrode shape on grounding resistances—Part 2: Experimental results and cryospheric monitoring. Geophysics, 81(1), pp.WA169-WA182
6. Zeeuw P.M. Wavelet and image fusion. CWI (1998). URL: https://groups.google.com/d/msg/comp.soft-sys.matlab/AjqIENmx1Z4/5g7QDFrZvWMJ
7. Li H., Manjunath B., Mitra S. Multisensor image fusion using the wavelet transform. Graph Models Image Process, 57 (3) (1995), pp. 235-245, 10.1006/gmip.1995.1022